Acacia senegal Gum: Continuum of Molecular Species Differing by Their Protein to Sugar Ratio, Molecular Weight, and Charges

Denis Renard,*,† Laurence Lavenant-Gourgeon,† Marie-Christine Ralet,† and Christian Sanchez‡

Unité de Recherches Biopolymères, Interactions, Assemblages, INRA, Rue de la Géraudière, BP 71627 44316 Nantes Cedex 3, France, and Laboratoire de Physico-Chimie et Génie Alimentaires, ENSAIA-INPL, 2 avenue de la Forêt-de-Haye, BP 172, 54505 Vandoeuvre-lès-Nancy, France

Received February 16, 2006; Revised Manuscript Received May 23, 2006

The main chemical and physical features of the *Acacia senegal* exudate gum and its molecular fractions isolated by chromatographies were determined using a wide variety of methods. Three main molecular fractions were isolated after hydrophobic interaction chromatography (HIC) and biochemical analyses confirmed the presence of an arabinogalactan-peptide (FI), an arabinogalactan-protein (FII), and a glycoprotein (FIII) fraction as described commonly in the literature. Further purification of FIII using size exclusion chromatography revealed three distinct populations. A wide molecular weight distribution within each population with the presence of at least two distinct molecular species per population was identified by high performance size exclusion chromatography coupled to on line multi-angle laser light scattering (HPSEC-MALLS). In addition, both sugars content (neutral and uronic acids) and UV profiles revealed that FIII was composed of a continuum of molecular species differing both by their protein-to-sugar ratio and molecular weight. FI and FII had average molecular weight $\bar{M}_w$ of 2.86×10^5 and 1.86×10^6 g·mol^{-1}, respectively, and a low polydispersity index ($M_w/M_n \sim 1.3$). The three populations identified in FIII after HIC separation had $\bar{M}_w$ of 2.67×10^6, 7.76×10^5, and 2.95×10^5 g·mol^{-1} and very low polydispersity indexes (1.13, 1.04, and 1.01). Estimation of the polypeptide backbone length in the three fractions gave 43, 2253, and 4443 amino acid residues, respectively, hydroxyproline (Hyp) and serine being the most prominent residues within FI and FII, Hyp and Asx (asparagine + aspartic acid) within FIII. Secondary structure prediction from circular dichroism data resulted in polyproline II, β-sheet, and random coil structures for FII and FIII, whereas no secondary structure was identified in FI. The existence of exposed tryptophanyl residues to the solvent was noticed by fluorescence in FII and FIII, tryptophan residues being absent from FI. In addition, 8−5′ non cyclic diferulic acid was identified to be covalently linked to carbohydrate moieties of FII. Infrared spectroscopy identified the different vibrations of saccharidic and peptidic bonds with absorbance amplitudes in agreement with sugar and protein elementary analyses. Titration measurements in order to evaluate the number of charges on total Acacia gum and its molecular fractions revealed that 100% of charges came from polysaccharidic moieties (i.e., glucuronic acids) in FI. Charges coming from polysaccharidic moieties were of 91.3% and 37.9% for FII and FIII, respectively, the remaining 8.7% and 62.1% charges in FII and FIII molecular fractions coming from the polypeptidic backbone.

1. Introduction

Exudate gums are among the oldest natural gums being used as thickening and stabilizing agents. Exudate gums are produced by many trees and shrubs as a natural defense mechanism, particularly in semiarid regions of Africa. When the plant's bark is injured, an aqueous gum solution is exuded to seal the wound, preventing infection and dehydration of the plant. The solution dries in contact with air and sunlight, to form hard, glasslike lumps which can easily be collected.[1] Exudate gums have been important items of international trade in the food, pharmaceutical, adhesive, paper, textile, and other industries for centuries. Today, Acacia gum is widely used for its nutritional, flavoring, and surface properties by the food industry,[2−6] in microencapsulation involving complex coacervation processes.[7−10]

Acacia gum (or gum arabic) is defined by the FAO/WHO Joint Expert Committee for Food Additives (JECFA) as: "a dried exudate obtained from the stems and branches of *Acacia senegal* (L.) Willdenow or *Acacia seyal* (Fam. Leguminosae)".[11] The Acacia gum is a branched, neutral or slightly acidic, complex polysaccharide obtained as a mixed calcium, magnesium, and potassium salt. The main chain consists of 1,3-linked β-D-galactopyranosyl units. The side chains are composed of two to five 1,3-linked β-D-galactopyranosyl units, joined to the main chain by 1,6-linkages. Both the main and the side chains contain units of α-L-arabinofuranosyl, α-L-rhamnopyranosyl, β-D-glucuronopyranosyl, and 4-*O*-methyl-β-D-glucuronopyranosyl, the latter two mostly as end-units.[12] Acacia gum would be composed by 64 ramified 1,3-linked homogalactan symmetrically arranged subunits, each of molecular mass 8000.[13]

Acacia gum is defined as an heteropolysaccharide since it contains about 2% of a polypeptide.[14] Acacia gum is also described as heteropolymolecular, because it has, on one hand, a variation in monomer composition and/or in the linking and

* Corresponding author. Tel.: 33 2 40 67 50 52. Fax: 33 2 40 67 50 25. E-mail: drenard@nantes.inra.fr.
† INRA.
‡ ENSAIA-INPL.

10.1021/bm060145j CCC: $33.50
Published on Web 08/05/2006

branching of the monomer units and, on the other hand, a molecular mass distribution. The consequence of this heterogeneity was reflected through the molecular species collected after fractionation of the gum and the mode of both separation and detection used.[15−19]

Using hydrophobic interaction chromatography (HIC), the bulk of the gum (88.4 wt % of the total) was shown to be comprised by the so-called arabinogalactan (AG) fraction with weight-average molecular weight ($\bar{M}_w$) of 2.79×10^5 g·mol^{-1} from light scattering measurements and low in protein (0.35 wt %).[17] The second major fraction (10.4 wt % of the total) was identified as an arabinogalactan−protein complex (AGP) with a molecular weight of 1.45×10^6 g·mol^{-1} and contained a greater proportion of protein (11.8 wt %). The third minor fraction (1.24 wt %) consisted of one, or possibly two, glycoproteins (GP). One of the GP had a molecular weight of 2.5×10^5 g·mol^{-1} and the highest protein content (47.3 wt %). The proteinaceous component of the first two fractions had similar amino acid distributions, with hydroxyproline and serine being the most abundant. The amino acid composition of the third fraction was significantly different with aspartic acid being the most abundant. Previous work using ^{1}H and ^{13}C NMR spectroscopy and methylation analysis showed that there were no major differences in the sugar constituents of the above three fractions.[20]

The tertiary structure of AGP has been described in terms of a "wattle blossom" macromolecular assembly by virtue of which few (∼5) discrete polysaccharide domains of $\bar{M}_w \sim 2 \times 10^5$ g·mol^{-1} are held together by a short peptide backbone chain.[21] An alternative model was proposed that described the gum Acacia glycoprotein (GAGP) as a "twisted hairy rope".[22] Using preparative gel filtration and electron microscopy, the authors concluded that the molecules had a polypeptide backbone with numerous small carbohydrate substituents linked through hydroxyproline residues. As the way to purify AGP and GAGP by the authors was different, hydrophobic interaction vs size exclusion chromatography, we may however wonder if a comparison between the "wattle blossom" and "twisted hairy rope" model to describe AGP molecules in Acacia gum is judicious. In addition, it was also surprising to notice that no model was proposed to describe the arabinogalactan fraction (AG). This fraction was identified by so far as the main fraction and could play a key role in the functional properties of the whole gum.

Previous work performed in the laboratory aimed to characterize both structure and rheological properties of Acacia gum dispersions.[23] Acacia gum molecules would display a random coil shape, whereas gum dispersions displayed solidlike mechanical properties during aging. This behavior would be related to the known surface properties of Acacia gum, in particular the ability of the gum to form elastic films at gas−liquid or liquid−liquid interfaces. A recent study on the mechanical properties of Langmuir monolayers at the air−water interface on Acacia gum and its fractions revealed that only GP fraction (i.e., the third fraction collected after HIC separation) developed greater surface pressure at the same surface per milligram of material than whole gum.[24]

The objectives of this work were to fractionate Acacia gum by hydrophobic interaction chromatography and further GP fraction by size exclusion chromatography in order to get enough material to conduct thorough structural and biochemical investigations. The molecular fractions and whole gum were identified by different chemical analyses (sugar, uronic acids, protein content, and amino acid composition). The determination of molecular weights and size distributions were performed by coupling on line to a high performance size exclusion chromatograph, a multi-angle laser light scattering detector (HPSEC-MALLS), a differential refractometer, a UV detector, and a differential viscosimeter. Other physical characterizations of the different fractions and the whole gum dealt with spectroscopic methods (UV−Vis, fluorescence, circular dichroism, and Fourier transform infrared) and titration measurements in order to get deeper insight into the tertiary molecular structure and charges distribution on Acacia gum and its fractions.

2. Material and Methods

2.1. Material. Acacia gum type from *Acacia senegal* trees (lot 97J716) was provided by the Colloïdes Naturels International Company (CNI, Rouen, France). As reported previously,[8] the powder contained 6.65% moisture and 3.1% ash (mineral content: 0.2% Mg^{2+}, 0.61% Ca^{2+}, 0.032% Na^+ and 0.9% K^+) and was further extensively dialyzed against distilled water and freeze-dried. The purity of Acacia gum was previously checked by ^{13}C NMR and was within JEFCA specifications.[25] In particular, only five major resonance peaks or sets of resonance peaks were found, corresponding to the carbonyl group on carbon C_6 of uronic acids (δ: 177 ppm), −CH groups located on carbon C_1 (δ: 115−110 ppm), −CH groups located on C_2 and C_5 positions in hexose rings (δ: 90−70 ppm), $-CH_2$ groups on carbon C_6 of hexoses residues (δ: 65 ppm), and $-CH_3$ group of rhamnose residues (δ: 20 ppm).

All other reagents were of analytical grade.

2.2. Preparation of Acacia Gum Dispersions. *Acacia senegal* gum dispersions were prepared by weight (wt %). Known amounts of Acacia gum powder previously dialyzed and freeze-dried were dispersed in the appropriate solvent conditions (depending on the method of separation or characterization used) under gentle stirring conditions at 25 ± 1 °C during 4−5 h. The dispersions were left at 4 ± 1 °C during at least 18 h to enable complete hydration of both Acacia gum and its fractions. The dispersions were centrifuged at 16 000 g for 40 min (T = 25 °C) to remove air bubbles and insoluble material.

2.3. Hydrophobic Interaction Chromatography (HIC). HIC was performed at room temperature on a Phenyl-Sepharose CL-4B (Pharmacia, Uppsala, Sweden) column (75 × 2.6 cm) equilibrated with degassed 4.2 M NaCl. Acacia gum (50 or 250 mL at 10 wt %) in 4.2 M NaCl was loaded and eluted successively by 4.2 M NaCl (fraction I), 2 M NaCl (fraction II), and finally water (fraction III) at a flow rate of 46.2 mL/h. A UV detector was used for continuous monitoring of absorbance at 280 nm. Fractions of 24 mL were collected and total neutral sugar and uronic acids quantified colorimetrically.[26,27] The appropriate fractions were pooled, extensively dialyzed against distilled water and freeze-dried for further analyses.

2.4. Size Exclusion Chromatography (SEC). Fraction III was further fractionated by SEC on a Sephacryl S-500 A (Pharmacia, Uppsala, Sweden) column (85 × 2.6 cm) using 0.5 M NaCl as eluent. The sample (2.5 mL at 10 wt %) was solubilized in water. NaCl (1 M) was added to give a final ionic strength of 0.5 M. The solution (5 mL) was loaded at a flow rate of 36 mL/h and the absorbance continuously monitored at 280 nm. Fractions of 4.8 mL were collected and analyzed for total neutral sugar, uronic acid, and absorbance at 214 nm. The appropriate fractions were pooled, extensively dialyzed against distilled water, and freeze-dried for further analyses.

2.5. Neutral Sugars Composition and Uronic Acids Content. Uronic acids and neutral sugars contents were determined colorimetrically by the automated *m*-phenylphenol methods,[26,27] respectively. Uronic acids were quantified in the presence of tetraborate. Individual neutral sugars were quantified after acid hydrolysis (trifluoro-acetic acid 2 M, 2 h, 121 °C) of total gum and its molecular fractions as their alditol acetates derivatives[28] by gas liquid chromatography using inositol as internal standard.

2.6. Nitrogen Content. The percentage of nitrogen was determined after digestion of the samples in concentrated sulfuric acid by an automated ammonia/salycilate reaction.[29] The method was slightly modified as follows: selenium was used as a catalyst and the digestion was performed at 300 °C for 2 h. The protein content was calculated using a conversion factor of 6.6 as proposed previously.[28] Two replicates were tested for each sample.

2.7. Amino Acid Analysis. After acid hydrolysis under vacuum in the presence of 6 N HCl for 24 h at 110 °C in a Pico-Tag Station (Waters), amino acids were derivatized with PITC[30] and analyzed on a C_{18} Pico-Tag column (0.39 id. x 15 cm, Waters). Dried samples were dissolved in 95% 2 mM Na_2HPO_4, pH 7.4, 5% acetonitrile. The HPLC column was equilibrated with buffer A (94% 0.14 M CH_3COONa containing 3.59 mM triethylamine pH 6.4, 6% acetonitrile), and the elution was performed with a convex gradient from 100% buffer A to 46% buffer B (40% H_2O/60% acetonitrile) in 10 min, at a flow rate of 60 mL/h. Both column and buffers were maintained at 38 °C and the absorbance was recorded at 254 nm. Each sample was replicated.

2.8. Identification of Phenolic Compounds. Phenolic compounds were determined by HPLC after saponification and extraction. The samples were saponified by 2 M NaOH at 35 °C under argon during 30 min in the dark. After an initial standard (3,4,5-trimethoxycinnamic acid) has been added, the solution was neutralized with 2 M HCl. Phenolic compounds were extracted with ether. The ether phase was evaporated at 40 °C, 1 mL of MeOH/H_2O (1:1, v/v) was added, and samples (20 μL) were injected on an HPLC system equipped with a C18 column (Purospher, Merck). Gradient elution was performed using MeOH/acetic acid (1:0.01) (A) and H_2O/acetic acid (1:0.01) (B) at 0.7 mL/min at 25 °C: (0 min, $A = 20\%$; 20 min, $A = 60\%$; 21 min, $A = 80\%$; 30 min, $A = 80\%$; 31 min, $A = 20\%$). Phenolic compounds were detected at 320 nm. Elution time and response factors relative to 3,4,5-trimethoxycinnamic acid at 320 nm were established using commercial ferulic acid and dehydroferulic acid standards as reported previously.[31]

2.9. Refractive Index Increment. The refractive index increment (dn/dc) was determined for the whole gum and its molecular fractions (concentration range: 0−0.5 wt %) in 0.05 M $NaNO_3$ buffer at 25 °C using a refractometer (Bellingham & Stanley Ltd., U.K.) illuminating the samples at a wavelength of 589 nm.

2.10. Molecular Mass Distribution and Intrinsic Viscosity. Acacia gum and its molecular fractions after HIC and SEC separations were analyzed by aqueous high performance size exclusion chromatography (HPSEC). Weight average molecular weight ($\bar{M}_w$) and number average molecular weight ($\bar{M}_n$) determinations were performed using a multi-angle laser light scattering (MALLS) setup (MiniDawn, Wyatt, Santa Barbara, CA) operating at three angles (41°, 90°, and 138°), an on-line differential viscosimeter (T-50A, Viscotek; universal calibration curve established with pullulans in the range $5-1600 \times 10^3$ g/mol), a UV detector, and a differential refractometer (RI; ERC 7547A). The refractive index increment (dn/dc) of Acacia gum and its molecular fractions determined experimentally were used and $\bar{M}_w$, $\bar{M}_n$ and the radius of gyration R_g were calculated using Astra 1.4 software (MALLS). The intrinsic viscosity [η] was calculated using TriSEC 3.0 software (Viscotek).

Acacia gum (0.1 wt %) and its molecular fractions (0.04 wt %) were prepared as described previously in 0.05 M $NaNO_3$ buffer containing 0.02% NaN_3 as preservative, and filtered through 0.2 μm Anotop membranes (Anotop, Alltech, France). HPSEC was performed at room temperature on a system constituted of one Shodex OH SB-G precolumn followed by two columns in series (Shodex OH−Pack SB-804 HQ and OH−Pack SB-805 HQ) eluted with 0.05 M $NaNO_3$ buffer containing 0.02% NaN_3 at a constant flow rate of 42 mL/h.

2.11. UV−Visible Spectroscopy. Acacia gum and its molecular fractions were characterized between 200 and 400 nm using a $\lambda 2$ double beam spectrophotometer (Perkin-Elmer, U.K.) equipped with a Peltier device. Measurements were carried out using 1 cm path length quartz cuvettes and a temperature of 25 °C. To take into account the differences in solubility for Acacia gum and its fractions, spectra were corrected for turbidity. The contribution of turbidity to the maximum UV absorption was obtained by extrapolation of the linear relation in bi-logarithmic coordinates of optical density against wavelength in the 400−360 nm region.

2.12. Circular Dichroism. The circular dichroic spectra of standard poly-L-hydroxyproline (10−30 kDa, MP Biomedicals), Acacia gum, and its molecular fractions were recorded on a CD6 Dichrograph Instrument (Jobin-Yvon, Longjumeau, France) at 25 °C, calibrated using ammonium d_{10}-camphorsulfonic acid. Spectra were averaged over two scans with a bandwidth of 1 nm and step resolution of 0.5 nm. All spectra were reported in terms of molecular ellipticity [θ] (deg·cm^2·dmol^{-1}) within the 185−260 nm spectral region using a 1-mm path-length cylindrical cuvette. Acacia gum, FI, FII, and FIII concentrations used (after filtration on 0.2 μm pore sizes) were of 4, 4, 2, and 0.3 wt %, respectively. The respective protein molar concentrations of each sample were of 75, 140, 10.8, and 1.96 μM (see Results for details). Poly-L-hydroxyproline was dissolved in water at 20 μM. All spectra were corrected for the solvent (water) obtained under identical conditions; noise reduction was applied according to the Jobin-Yvon software. CD spectra acquisition was repeated twice.

CD spectra of FII and FIII were analyzed in terms of secondary structure content by using the Dichroprot software,[32] a package freely available online (http://dicroprot-pbil.ibcp.fr). The Self-consistent method (SCM) for estimating the secondary structure content, in particular the polyproline II (PPII) type conformation, was used. In this method,[33] the spectrum of the protein to be analyzed is included in the basis set and an initial guess is made for the unknown structure as a first approximation. The resulting matrix equation is solved using the singular value decomposition algorithm and the initial guess is replaced by the solution. The process is repeated until self-consistency is attained. The best features of the variable selection and the locally linearized methods are incorporated into the procedure. In the Dichroprot software, the prediction for secondary structure content is calculated from four reference databases.

2.13. Intrinsic Fluorescence Spectroscopy. The fluorescence spectra of Acacia gum and its fractions were recorded on a Spex Fluoromax (Jobin-Yvon, Longjumeau, France) at 25 °C using an excitation wavelength of 290 nm. Spectra were collected with a step resolution of 1 nm and emission and excitation slits fixed at 4 nm. All spectra were corrected for the solvent in the 300−500 nm region using a 1-cm path length. Acacia gum, FI, FII, and FIII concentrations used (after filtration on 0.2 μm pore sizes) were of 4, 4, 0.7, and 0.3 wt %, respectively. Spectra recording was repeated four times.

2.14. Fourier Transform Infrared Spectroscopy (FTIR). FTIR spectra of thin dry films of Acacia gum and its fractions were obtained on a tensor 27 FTIR spectrophotometer (Bruker Optics, Kalsruhe, Germany). Thin dry films were obtained from mixtures of freeze-dried powders and KBr using a manual pellet press (Specac, Orpington, U.K.) and mounted on a QuickLock base plate. A total of 64 scans between 400 and 4000 cm^{-1} were recorded at 4 cm^{-1} resolution on the transmission mode using a DTGS detector. Raw absorbance spectra were baseline corrected, smoothed using a 9 points Savitsky-Golay function, and Min-Max normalized. Second derivative spectra were obtained while using a 9 points Savitsky-Golay function. Spectra acquisition was repeated three times, each time with freshly prepared thin dry films.

2.15. Potentiometric Measurements. Acacia gum and its fractions (160 mg in 10 mL water) were prepared as described in section 2.2. Percolating the samples through a strong H^+-exchanger (Rohm & Haas Amberlite IR 120) allowed the recovery of Acacia gum and its fractions in the acidic form at a concentration of (C_p) ~ 3 mg/mL. Titration measurements (sample volume: 24 mL) were performed at $T = 25$ °C with an automated titrator TitraLab 90 (Radiometer Analytical, Copenhagen, Denmark) using freshly prepared 0.01 N NaOH solution. Each titration measurement was repeated three times. Glucuronic, aspartic, and glutamic acids were also titrated for comparison at concentrations of 0.2 mg/mL.

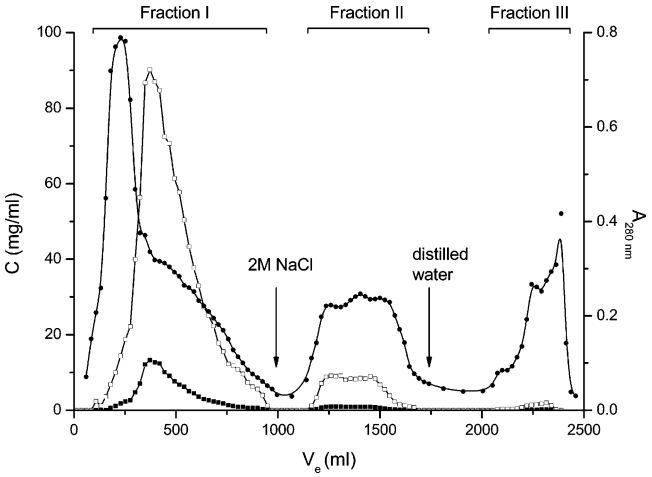

Figure 1. Elution curve of Acaciagum (25 g in 225 mL of 4.2 M NaCl) following fractionation by hydrophobic interaction chromatography on Phenyl-Sepharose CL-4B. Molecular fractions were eluted using 4.2 M NaCl (808 mL), 2 M NaCl (808 mL), and distilled water (1215 mL). Left traces: neutral sugars (□) and uronic acids (■) concentration *C* (mg/mL). Right trace: A_{280nm} (●).

From the degree of neutralization α′ and the pH value for each neutralization step, the degree of dissociation α and the apparent p*K* (pK_a) of the gum and its fractions were calculated according to eqs 1 and 2

$$\alpha = \alpha' + \frac{[H^+]}{C_p} \quad (1)$$

$$pK_a = pH + \log\left(\frac{1-\alpha}{\alpha}\right) \quad (2)$$

3. Results and Discussion

Fractionation using Hydrophobic Interaction Chromatography (HIC). The fractionation of Acacia gum using HIC is given in Figure 1 where three major fractions denoted fractions I (FI), II (FII), and III (FIII) were eluted from the column using 4.2 M NaCl, 2 M NaCl, and distilled water, respectively. The UV profile obtained by monitoring the absorbance of the eluent at 280 nm and the sugar profiles (neutral sugars and uronic acids) obtained by measuring the concentrations in each collected tube showed that FI, FII, and FIII corresponded to very broad protein and sugar distributions and that they differed mainly by their sugar-to-protein ratio, the highest ratio being for FIII. On the contrary, the uronic acids to neutral sugar ratio differed slightly from one fraction to the other: 0.15, 0.11, and 0.09 were found for FI, FII, and FIII, respectively.

Several fractionations were performed in order to get sufficient material for further physicochemical studies and profiles similar to those presented in Figure 1 were recorded. Highly reproducible results were thus found for FI and FII purification. However, in some cases, UV profile at 280 nm revealed two distinct peaks for FIII. Previous literature data reported the existence of two peaks for FIII denoted fractions IIIA and IIIB using HIC separation.[34,35] All of the collected fractions corresponding to FI, FII, and FIII were pooled, extensively dialyzed against distilled water, freeze-dried, and then characterized using HPSEC-MALLS. By this way, the average molecular weights distribution gave information about the efficiency of the method of fractionation and the necessity or not to pursue the purification.

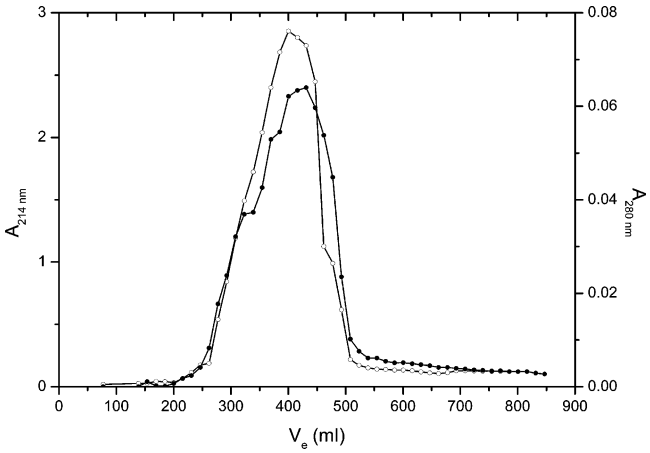

Figure 2. Elution curve of pooled molecular fraction I (8.15 g in 75 mL of 4.2 M NaCl) following fractionation by hydrophobic interaction chromatography on Phenyl-Sepharose CL-4B. Molecular fraction I was eluted using 4.2 M NaCl and the eluent was detected at 214 nm (○) and 280 nm (●).

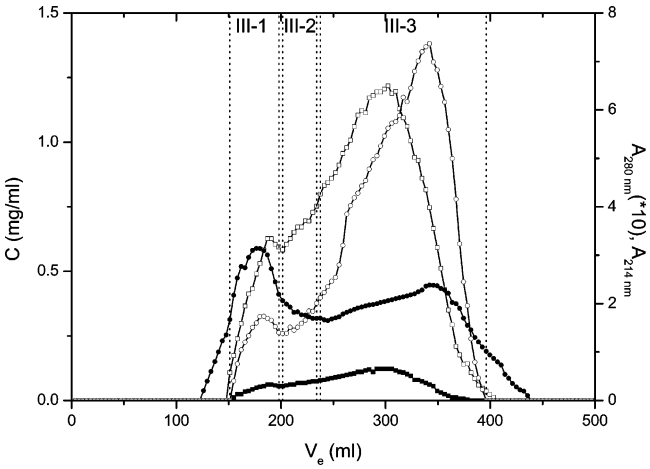

Figure 3. Elution curve of pooled molecular fraction III (250 mg in 5 mL of 0.5 M NaCl) following fractionation by size exclusion chromatography on Sephacryl S-500. Eluent was detected by measuring neutral sugars (□) and uronic acids concentration (■) and by monitoring the absorbance at 214 nm (○) and 280 nm (●). $A_{280\,nm}$ was magnified by a factor 10.

It was thus noticed for FI that two populations were detected based on light scattering, differential refractometer, and UV detections. The first population, corresponding to 2−4% of the total mass injected, had a $\bar{M}_w = 3.61 \times 10^6$ g/mol and a polydispersity $\bar{M}_w/\bar{M}_n = 1.14$, whereas the second population, corresponding to 98−96% of the total mass injected, had a $\bar{M}_w = 3.08 \times 10^5$ g/mol and a $\bar{M}_w/\bar{M}_n = 1.28$. These results were in agreement with the thin peak and the shoulder clearly identified by monitoring absorbance at 280 nm in Figure 1 in the elution volume region ranging from 0 to 1000 mL.

Similar results were obtained for FIII where three populations were identified by HPSEC-MALLS. The first population, corresponding to 47% of the total mass injected, had a $\bar{M}_w = 2.65 \times 10^6$ g/mol and a polydispersity $\bar{M}_w/\bar{M}_n = 1.12$, the second population, corresponding to 27.7% of the total mass injected, had a $\bar{M}_w = 7.90 \times 10^5$ g/mol and a $\bar{M}_w/\bar{M}_n = 1.04$, whereas the third population, corresponding to 25.3% of the total mass injected, had a $\bar{M}_w = 2.95 \times 10^5$ g/mol and a $\bar{M}_w/\bar{M}_n = 1.01$.

Without any consideration of the nature of each molecular species identified in FI and FIII, further fractionations using HIC separation for FI and SEC separation for FIII were performed in order to get homogeneous material on an average

Table 1. Chemical Analyses of Acacia Gum and Its Molecular Fractions Resulting from Hydrophobic Interaction Chromatography (HIC) and Size Exclusion Chromatography (SEC)

		fraction					
	total gum	I[a]	II	III	III-1[b]	III-2[b]	III-3[b]
yield[c] (%)		88.3	10.4	1.3	9.8	5.7	84.5
rhamnose (%)	11.3	11.9	7.4	7.3	6.8	5.9	5
fucose (%)	0.8	0.6	0.6	1.2	0.5	0.6	1
arabinose (%)	26	24.9	26.1	20.8	16.7	17.4	16.6
xylose (%)	0	0	0	0.5	0.2	0.2	0.5
mannose (%)	0	0	0	1.5	0.5	0.4	1.5
galactose (%)	44	44	34.8	27.5	22.7	22.2	0
glucose (%)	0	0.8	0	0.4	0.7	0.5	22.4
uronic acids (%)	15.4	15.6	11.8	8.8	2.5	0.2	0.5
protein (%)	2.4	1.1	9	24.6	n.d.[d]	n.d.	35.5
total % weight	99.9	98.9	89.7	92.6	50.6	47.4	83

[a] Fraction I resulting from two HIC separations. [b] Fractions III resulting from both HIC and SEC separations. [c] Corresponding to the material collected after one HIC separation (total gum and fractions I, II, and III) or collected after both HIC and SEC separations (fractions III-1, III-2, and III-3). [d] Not determined.

Table 2. Amino Acid Composition (Values Given in Residues/1000 Residues) of Acacia Gum and Its Molecular Fractions Resulting from Hydrophobic Interaction Chromatography (HIC) and Size Exclusion Chromatography (SEC)

amino acid	total gum	fraction I[a]	fraction II[b]	fraction III[b]	fraction III-3[c]
Hyp	229	258	340	121	112
Asx	48	61	32	109	104
Thr	72	86	78	54	58
Ser	108	147	122	104	123
Glx	47	43	33	67	64
Pro	72	65	62	57	59
Gly	55	61	42	80	85
Ala	44	43	23	47	48
Cys (R−SH)	0	3	0	9	6
Val	46	32	30	60	56
Met	0	3	0	6	5
Ile	33	15	17	21	23
Leu	68	61	64	75	73
Tyr	13	4	16	49	42
Phe	40	10	28	53	49
His	61	39	80	35	35
Lys	34	18	20	36	39
Arg	30	49	16	16	19
% protein[d]	2.3	1.0	8.9	24.5	32.6
% protein[e]	2.4	1.1	9	24.6	35.5

[a] Fraction I resulting from two HIC separations. [b] Fractions resulting from one HIC separation. [c] Fraction resulting from both HIC and SEC separations. [d] % protein calculated by summing the amino acids recovered. [e] % protein from Kjeldahl, using an N conversion factor of 6.60.

molecular weights distribution basis. Detailed molecular characteristics of the homogeneous purified fractions included FII will be given hereafter.

Purification of FI and FIII using Hydrophobic Interaction Chromatography (HIC) or Size Exclusion Chromatography (SEC). FI collected after the first HIC fractionation (from 60 to 948 mL) was re-solubilized in 4.2 M NaCl and fractionated again using the same support. The elution was performed using 4.2 M NaCl, and Figure 2 displayed UV profiles obtained by monitoring absorbance of the eluent both at 214 and 280 nm. Whatever the wavelength used, only one major peak was observed. The material within the major peak was further collected, extensively dialyzed against distilled water, and freeze-dried. The sugar analysis, protein content, and HPSEC-MALLS characterization were done on this purified FI.

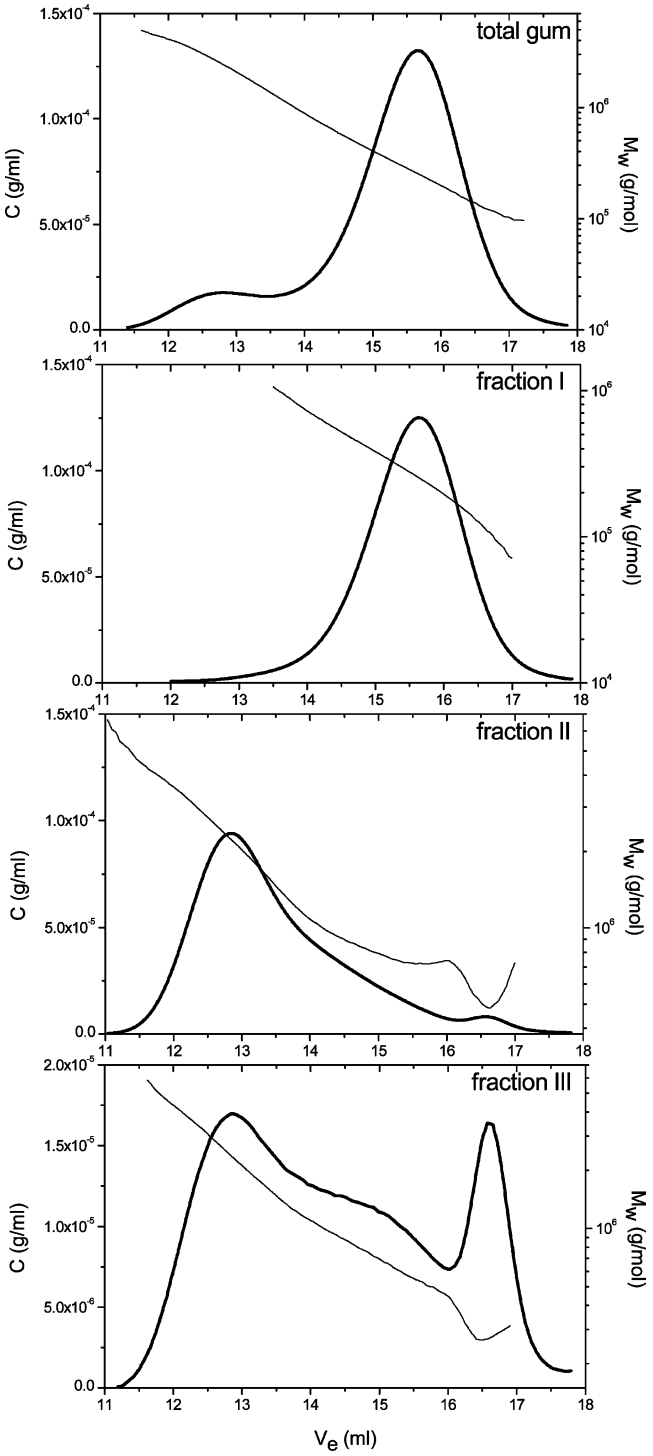

Figure 4. High performance size exclusion chromatography (HPSEC) chromatograms showing the elution profiles monitored by refractive index (*C*, g/mL) and light scattering (M_w, g/mol) for Acacia gum and its molecular fractions collected after hydrophobic interaction chromatography; refractive index (thick line) and light scattering (thin line).

FIII was re-solubilized in 0.5M NaCl and fractionated using SEC on a Sephacryl S-500 column. Figure 3 displayed the neutral sugar and uronic acids concentration profiles together with the UV profiles monitored both at 214 and 280 nm. The results showed that at least two populations differing in their sugar-to-protein ratio seemed to be distinguished. In addition, the uronic acids over the neutral sugars ratio were ~0.10

Table 3. Molecular Parameters of Acacia Gum and Its Molecular Fractions Resulting from Hydrophobic Interaction Chromatography (HIC) as Determined by High Performance Size Exclusion Chromatography Coupled On-Line to Multi Angle Laser Light Scattering (HPSEC-MALLS) and Differential Refractometer and Viscosimeter

	total gum		fraction I[a]	fraction II[b]	fraction III[b]		
	first population (11.3−13.3 mL)	second population (14.3−17.1 mL)	(13.8−17.2 mL)	(11.5−15.6 mL)	first population (11.5−13.6 mL)	second population (14.2−15.6 mL)	third population (16.3−17.3 mL)
C area (%)	11.5	88.5	100	97.4	48.5	31.0	20.5
d*n*/d*c*	0.147		0.145	0.171		0.153	
M_w g·mol^{-1} [c]	2.69×10^6	3.06×10^5	2.86×10^5	1.86×10^6	2.67×10^6	7.76×10^5	2.95×10^5
M_n g·mol^{-1} [c]	2.30×10^6	2.44×10^5	2.23×10^5	1.40×10^6	2.36×10^6	7.46×10^5	2.92×10^5
M_w/M_n	1.17	1.25	1.28	1.33	1.13	1.04	1.01
R_g nm	35.3	11.8[d]	11.3[d]	30	41.3	25.3	19.5
[η] mL·g^{-1} [e]	80.2	17.3	16.2	70.7	102.6	64.4	29.8
R_h nm (QELS)[f]	←——10.7——→		9.1	34.4	←——16.1——→		

[a] Fraction resulting from two HIC separations. [b] Fractions resulting from one HIC separation. [c] By HPSEC-MALLS. [d] R_g value calculated using the Flory−Fox equation [η] $M_w = 6^{3/2}\Phi R_g^3$ where Φ is the Flory viscosity constant ($\sim 2.2 \times 10^{23}$). [e] By differential viscosimetry. [f] Hydrodynamic radius determined by quasi-elastic light scattering at three angles (30, 90, and 150°) in 0.05 M NaNO3 buffer

whatever the population considered and were found to be very similar to the FIII isolated after HIC separation. For sugar analysis, protein content, and HPSEC-MALLS characterization, material eluted from SEC separation was separated into three fractions denoted III-1, III-2, and III-3 corresponding to 151−198 mL, 201.6−234 mL, and 237.6−396 mL elution volume ranges, respectively. In addition, SEC purification of FIII revealed a systematic shift between UV and sugar profiles during elution of the material and would tend to demonstrate that a continuum in molecular species would exist in this fraction. The absence of UV and sugar profiles superimposition during SEC elution of FIII would also mean that each fraction collected (III-1, III-2, and III-3) could be composed of different populations differing in molecular weight and polydispersity.

Sugars Composition, Protein Content, and Amino Acid Analysis. The neutral sugars, uronic acids composition, and protein content of Acacia gum and its molecular fractions were given in Table 1. The weights recovered for each fraction after one HIC separation were of 88, 10, and <2% for respectively FI, FII, and FIII, yields in agreement with earlier findings.[17,34] The sugar composition revealed a majority of arabinose (Ara) and galactose (Gal) for the whole gum and its fractions, the Ara/Gal ratio values being 0.59, 0.57, 0.75, and 0.76 for total gum, FI, FII, and FIII, respectively. Similar Ara/Gal ratio values were found for FIII-1 and FIII-2 with an exception for FIII-3 where no galactose was detected. The uronic acids content was quite low and very similar for total gum and FI (~15%), whereas it was quite negligible for FIII isolated after HIC and SEC fractionations. The uronic acids content for the whole gum, FI, and FII made these polysaccharides to be considered as weakly charged polyelectrolytes.

FI, which made up the bulk of the Acacia gum, contained a small proportion of proteinaceous material, whereas the minor FII and FIII contained comparatively high proportions of protein, in agreement with earlier findings.[17,34] The protein to total sugar ratio values were of 0.025, 0.022, 0.112, 0.362, and 0.747 for respectively whole gum, FI, FII, FIII, and FIII-3.

The amino acid composition of the whole gum and its fractions was reported in Table 2. Sulfur amino acids (methionine, cysteine) were also quantified, whereas Asx and Glx meant simply that the method used to determine the amino acid composition was not able to distinguish between the acidic and basic forms of these residues. As reported in the literature for many years, Acacia gum and its fractions were hydroxyproline-rich heteropolysaccharides with most of the carbohydrate attached to the polypeptide backbone as small hydroxyproline (Hyp)-polysaccharide substituents.[22,36] These results were confirmed in Table 2 where hydroxyproline (Hyp) and serine (Ser) were the most abundant amino acids contained in total gum, FI, and FII. Hyp and Asx (asparagine + aspartic acid) were the most abundant amino acid contained in FIII.

Molecular Mass Distribution and Intrinsic Viscosity of Acacia Gum and Its Molecular Fractions. The elution profiles of total gum and its fractions using HPSEC coupled to on-line differential refractometer, viscosimeter, and multi-angle light scattering (MALLS) were given in Figure 4 (concentration signal derived from the differential refractometer and molecular mass derived from light scattering were given). The Acacia gum profile displayed two distinct populations where the first peak reflected a small fraction of the whole gum sample (11.5%, Table 3) but scattered the light with a high intensity (data not shown) indicating the presence of very large molecular weight species. On the contrary, the second peak represented the major part of the sample (88.5%, Table 3), and the scattered light intensity was relatively smaller compare to the first peak (data not shown). This clearly demonstrated that the second population was composed of smaller molecular weight species. These results on Acacia gum were reported several times in the literature, and some discrepancies may exist from one publication to another due to essentially the elution volume range considered to integrate the different peaks.[37−40]

To our knowledge, no HPSEC-MALLS data were reported in the literature on the purified fractions obtained after HIC separation. Only average molecular masses from GPC data or from static light scattering and hydrodynamic radii from dynamic light scattering were reported in the literature on purified fractions collected after HIC separation.[17,24]

Figure 4 demonstrated that the FI refractive index elution profile was superimposed to the second population concentration signal of total gum. FII concentration signal covered partly the signal from the first population of total gum with, however, a slight shift in the maximum peak toward higher elution volume. In addition, an asymmetric distribution of FII was detected pointing out the high molecular weight polydispersity of this fraction. FIII was characterized by a much more polydisperse concentration signal that was divided into three distinct populations. In addition, molecular species identified at elution volume $V_e > 16$ mL for both FII and FIII displayed anomalous

molecular mass elution profiles. The molar mass of the eluting molecules increased with increasing elution volume in contradiction to the normal size exclusion separation mechanism. This anomalous behavior was however encountered in both cases of branched polymers and polymers having cylindrical shape.[41] Moreover, rigid rodlike molecules such as extensins (hydroxyproline-rich glycoproteins) were found to reptate into porous gel matrixes, resulting in a retardation different from that predicted by the mass of the macromolecule.[42] Table 3 summarized both static ($\bar{M}_w$, $\bar{M}_w/\bar{M}_n$, and R_g) and dynamic ([η] and R_h) molecular parameters of Acacia gum and its fractions. As each molecular fraction contained in Acacia gum differed in protein and sugar contents, the refractive index increment of the total gum and each purified fraction was previously measured in order to get accurate molecular mass determination. The value measured at $\lambda = 589$ nm for Acacia gum, $dn/dc = 0.147$, was found to be in total agreement with values reported in the literature at other wavelengths. A $dn/dc = 0.150$ at $\lambda = 546$ nm was found for the whole gum in acidic form,[43] whereas a $dn/dc = 0.141$ at $\lambda = 632.8$ nm was given for both total gum and FI.[17] To our knowledge, no data were available in the literature concerning FII and FIII.

From Table 3, it appeared that $\bar{M}_w$ values ranged from 2.86×10^5 to 2.67×10^6 g/mol and R_g values from 11.3 to 41.3 nm for FI and the first population of FIII, respectively. In the case of low $\bar{M}_w$ species, the radius of gyration was calculated using the Flory−Fox equation that makes the important assumption that the polymer is considered to be a random coil in good solvent. R_g values calculated in the case of the second population of the whole gum and FI should thus be taken with caution. The polydispersity index found in the third population of FIII was surprisingly very low for biopolymers where $\bar{M}_w/\bar{M}_n$ higher than 2 are very common. This molecular characteristic could reflect relevant biological function for this class of molecules.

The high polydisperse concentration signal obtained for FIII after HIC separation motivated a new separation using SEC where three fractions, denoted III-1, III-2, and III-3, were identified and collected (see Figure 3). Results from HPSEC-MALLS are displayed in Figure 5 where the three fractions revealed again high polydisperse concentration signals. Each signal was divided into three distinct populations in order to integrate peaks and get molecular parameters. In addition, as reported previously, the molar mass of the eluting molecules increased with increasing elution volume for $V_e > 16$ mL highlighting the hypothetical branched and/or cylindrical shape of the molecules. The relative content of this peculiar molecular species increased from 25.3% after HIC separation to 31.5% after HIC and SEC separations in FIII-3. Table 4 summarized both static and dynamic molecular parameters of FIII-1, FIII-2, and FIII-3 purified after both HIC and SEC separations. Very similar molecular parameters for each population were obtained whatever the fractions considered except maybe those found in FIII-3. Molecular weights and radii of gyration of both first and third population differed noticeably from those identified in FIII-1 and FIII-2. Further detailed analysis using HPSEC-MALLS and/or other scattering techniques will be needed to clearly distinguish each molecular species identified in FIII. HPSEC-MALLS data collected on FIII would tend to confirm that a continuum in molecular species would exist in this fraction.

Spectroscopic characterizations of total Acacia gum and its molecular fractions. The objectives were to characterize thoroughly Acacia gum and its molecular fractions using four spectroscopic techniques, UV−visible, circular dichroism, fluorescence, and Fourier transform infrared, to get deeper insight into the tertiary structure of these complex heteropolymers. In addition, more structural details on the polypeptidic backbone contained in each molecular fraction were searched in these spectroscopic investigations.

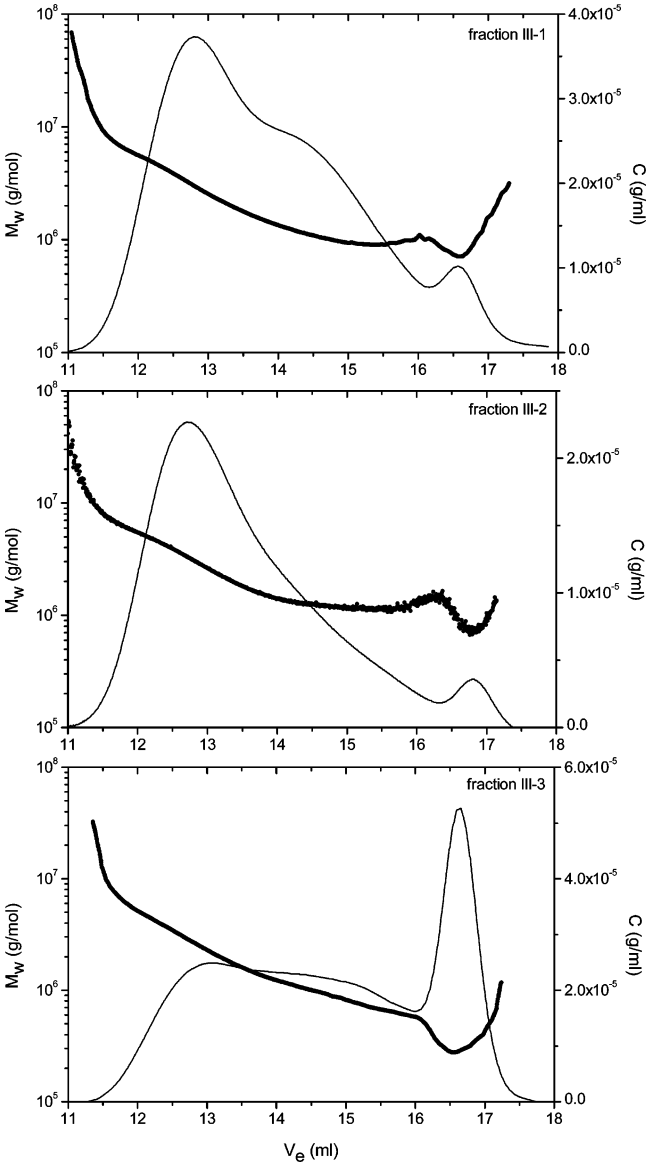

Figure 5. High performance size exclusion chromatography (HPSEC) chromatograms showing the elution profiles monitored by refractive index (*C*, g/mL) and light scattering (M_w, g/mol) for molecular fraction III collected after both hydrophobic interaction chromatography and size exclusion chromatography; refractive index (filled line) and light scattering (symbols).

UV−Vis Spectroscopy. Acacia gum and its purified fractions were first characterized using UV−Vis spectroscopy where the amino acids composition (presence of aromatic residues such as Phe and Tyr, Trp being not quantified) and the protein content allowed the UV signature of each molecular species to be analyzed. Figure 6 displayed the UV−Vis spectra recorded between 245 and 345 nm for Acacia gum and its fractions together with the second derivative spectra. Total gum and FIII spectra displayed a maximum at $\lambda = 277$ nm, whereas the FII spectrum revealed a maximum at $\lambda = 274$ nm. In addition, total gum, FII, and FIII displayed a shoulder at 281 nm. No true maximum and shoulder in absorbance were noticed for FI. The addition of 8 M urea revealed however a small peak and shoulder in the absorption spectrum located at $\lambda = 276$ and

Table 4. Molecular Parameters of the Different Populations Identified by High Performance Size Exclusion Chromatography Coupled On-Line to Multi Angle Laser Light Scattering (HPSEC-MALLS) Contained in the Acacia Gum Molecular Fraction III and Resulting from Both Hydrophobic Interaction Chromatography (HIC) and Size Exclusion Chromatography (SEC)

	fraction III-1			fraction III-2			fraction III-3		
	first population (11.6−13.6 mL)	second population (14.2−15.7 mL)	third population (16.3−17.0 mL)	first population (11.5−13.6 mL)	second population (14.0−15.9 mL)	third population (16.4−17.2 mL)	first population (11.5−13.7 mL)	second population (14.0−15.7 mL)	third population (16.2−17.2 mL)
relative content (%)	61.2	32	6.8	67.8	27.7	4.5	35.5	33.0	31.5
$[\eta]$ mL·g^{-1} [a]	79.3	42.9	12.4	nd[b]	nd	nd	79.2	44.0	8.0
M_w g·mol^{-1} [c]	3.38×10^6	1.02×10^6	8.87×10^5	3.50×10^6	1.29×10^6	9.93×10^5	2.86×10^6	8.98×10^5	3.34×10^5
M_n g·mol^{-1} [c]	2.91×10^6	1.01×10^6	8.43×10^5	3.04×10^6	1.28×10^6	9.26×10^5	2.43×10^6	8.67×10^5	3.23×10^5
M_w/M_n	1.16	1.01	1.05	1.15	1.00	1.07	1.17	1.04	1.04
R_g nm	40.0	35.9	52.0	45.4	35.0	48.0	43.8	28.0	26.0

[a] By differential viscosimetry. [b] Not determined. [c] By HPSEC-MALLS using dn/dc = 0.153.

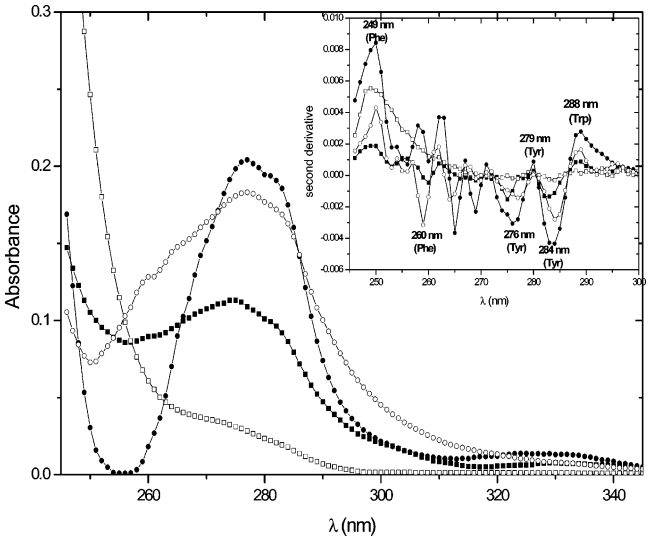

Figure 6. UV−Visible spectra corrected for turbidity of Acacia gum (C = 2%, w/v) and molecular fractions I (C = 2%, w/v), II (C = 2%, w/v), and III (C = 0.3%, w/v) solutions in water obtained after hydrophobic interaction chromatography; (inset) second derivative spectra of total gum and its molecular fractions pointed out the maxima and minima in the UV spectral region of phenylalanine (Phe), tyrosine (Tyr), and tryptophan (Trp) residues. (■) total gum; (□) fraction I; (●) fraction II; (○) fraction III

282 nm, respectively (data not shown). From amino acids composition, the aromatic residues percentages (Phe + Tyr) were evaluated to be of 5.3, 1.4, 4.3, and 10.3 for total gum, FI, FII, and FIII, respectively. From these percentages and UV−Vis spectra, FI could be considered to have no tryptophan (Trp) residues in its sequence as revealed by the absence of a maximum and shoulder in the absorption profile. Another hypothesis would be that the aromatic residues would be totally buried in the molecule, the exposition of these amino acids to the solvent being achieved using 8 M urea.

Second derivative spectra clearly identified maxima and minima of aromatic residues in the UV spectral region for all samples. In particular, a maximum at λ = 249 nm and a minimum at λ = 260 nm were noticed for Acacia gum and its fractions, wavelength characteristic of Phe residue absorption. The minimum at 260 nm was however absent of the FI spectrum. Two minima located at λ = 276 and 284 nm and a maximum at λ = 279 nm, characteristic of Tyr residue absorption, were noticed for total Acacia gum, FII, and FIII. These above-mentioned minima and maximum were however not identified in the FI absorption spectrum, even in the presence of 8 M urea, due to the very low aromatic residues content. Finally, a maximum at λ = 288 nm was noticed for total gum, FII, and FIII, wavelength characteristic of Trp absorption. These UV−Vis absorption spectra gave complimentary qualitative information to amino acids analysis in the sense that Trp residues were found to be mainly present in total Acacia gum, FII and FIII.

Far-UV Circular Dichroism. The second characterization of Acacia gum and its fractions dealt with far-UV circular dichroism (CD) in order to probe the secondary conformational state in solution of these hydroxyproline-rich heteropolysaccharides. First, calculations were performed in order to estimate the relative protein concentration (relative C_{prot}) in each sample based on both protein content (protein %) and concentration used for CD measurements (C_{CD}). The knowledge of the relative C_{prot} and the protein molecular weight (M_{prot}) contained in each molecular fraction allowed the CD signal to be converted into molecular ellipticity $[\theta]$ (deg·cm^2·dmol^{-1}). Calculations were performed using the basic relationships

$$\text{relative } C_{prot} = C_{CD}, \%\text{protein} \quad (3)$$

$$M_{protein} = (\bar{M}_w, \text{mol } \%\text{protein}) \quad (4)$$

$$\text{number of residues} = M_{protein}/M_{residue} \quad (5)$$

with $\bar{M}_w$, the weight average molecular weight of each fraction (see Tables 3 and 4) and $M_{residue}$, the average residue molecular weight calculated from amino acid composition of each fraction (see Table 2). Table 5 summarized the relative protein concentration corresponding to the concentrations used for CD measurements, the protein molecular weight, and the number of amino acids residues for total gum and each population identified in the molecular fractions.

The average number of amino acids residues would be of 43, 2253, 4443, and 6333 for FI, FII, FIII, and FIII-3, respectively. The number of residues in particular for FIII and FIII-3 was considered to be a rough estimation considering the different populations identified by HPSEC-MALLS.

Figure 7 displayed the far-UV CD spectra in the 185−260 nm region of Acacia gum and the three fractions. A polyhydroxyproline standard was also displayed for comparison. A minimum in the mean residue ellipticity was clearly identified for total gum, FII, and FIII at respectively 207, 203.5, and 205 nm. In addition, a maximum in ellipticity was noticed at 226 nm for total gum, FII, and FIII. The minimum and maximum identified for total gum, FII, and FIII were much less pronounced

Table 5. Relative Protein Concentration (C_{prot}) of Acacia Gum and Its Molecular Fractions (Collected after Hydrophobic Interaction Chromatography (HIC) and Size Exclusion Chromatography (SEC)) Calculated from Both Concentrations Used for Circular Dichroism Measurements (C_{CD}) and Protein Content (%)[a]

	total gum	fraction I[b]	II[c]	III[c]	III-3[d]
protein (%)[e]	2.4	1.1	9.0	24.6	35.5
C_{CD} (%, w/v)	4	4	2	0.3	
relative C_{prot} (%, w/v)	0.096	0.044	0.175	0.0738	
M_{prot} (g/mol)	17836	4607	247358	483851	683302
no. of residues	164	43	2253	4443	6333

[a] Protein molecular weight (M_{prot}) and average number of amino acid residues (using an average residue molecular weight calculated from amino acid composition) of each molecular fraction were also given. [b] Fraction I resulting from two HIC separations. [c] Fractions resulting from one HIC separation. [d] Fraction resulting from both HIC and SEC separations. [e] % protein from Kjeldahl using an N conversion factor of 6.60.

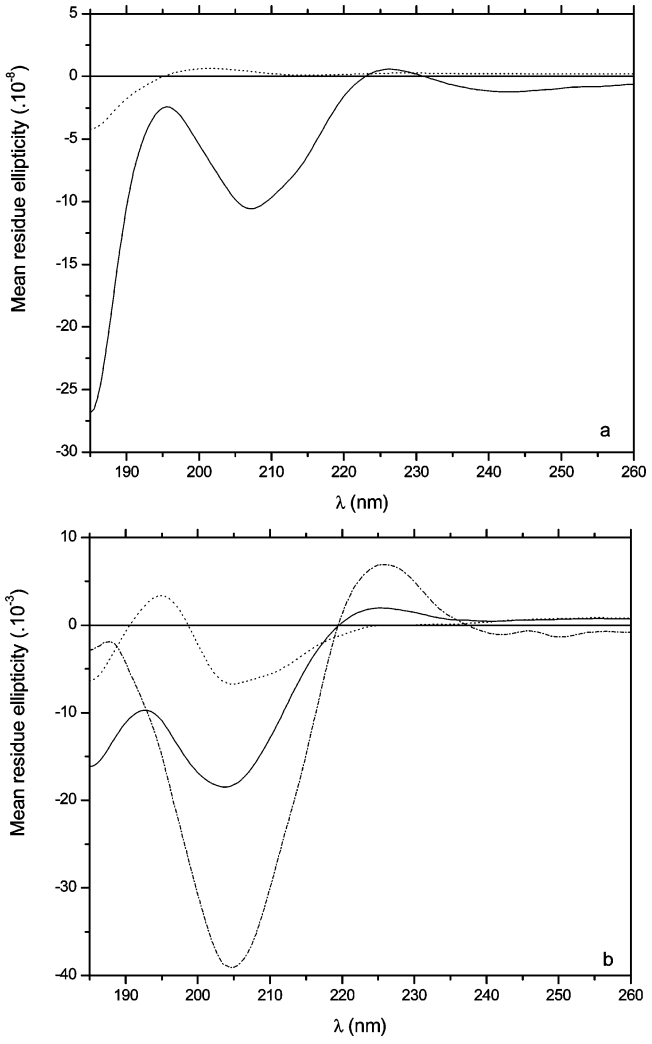

Figure 7. Far-UV CD spectra of Acacia gum and molecular fraction I (a), fractions II, III, and polyhydroxyproline standard (b) solutions in water obtained after hydrophobic interaction chromatography. Samples were dissolved in water at a relative protein concentration of 75 and 140 μM for total gum and molecular fraction I (a), respectively; 10.8, 1.96, and 20 μM for molecular fractions II, III, and polyhydroxyproline standard, respectively. (a) total gum (—), fraction I (- - -); (b) fraction II (—), fraction III (- - -), and polyhydroxyproline (–·–·)

in the case of FI. This result would be in agreement with both low amino acids content and low aromatic residues percentage included in FI. In addition, the low marked minimum and maximum in ellipticity identified in FI compared to FII and FIII were shifted toward higher wavelengths at 215 and 227.5 nm, respectively. The curve with large amplitudes in Figure 7b with a minimum at 205 nm and a maximum at 226 nm corresponded to the polyhydroxyproline standard in the polyproline II (PPII) conformation, a left-handed helix with three residues/turns and a pitch of 0.94 nm.[44] This PPII type conformation would be partially adopted by the total gum, FII and FIII in solution. CD secondary structure analyses of FII and FIII, using Dichroprot software, predicted 27% and 9% PPII type conformation, respectively, but also a significant amount of β-sheet and unordered (random coil) structure. The presence of the oligosaccharide side chains would impose some sterical constraints to the whole molecule that would deform the polypeptide backbone. This hypothesis was confirmed by the random coil conformation also adopted by both fractions. The presence of a higher arabinoside content in FII compare to FIII shifted the spectrum minimum from 205 to 203.5 nm. This result was previously established in the case of both arabinogalactan protein from tomato[45] and synthetic glycoprotein $(Ala\text{-}Hyp)_{51}$ after deglycosylation.[46]

A second minimum appeared for all of the samples around 185 nm. It was demonstrated that the glycosylated molecules, particularly hydroxyproline-rich glycoproteins (HRGPs) containing arabinogalactan polysaccharide substituents, always displayed a minimum at 183 nm.[47] In addition, the decrease of carbohydrate content from FI to FIII was accompanied by a decrease in the net intensities of its extrema, with molar ellipticities ranging from 9.6×10^6 to -6700 deg·cm^2·dmol^{-1} for the minimum at ~205 nm and from 2.74×10^7 to -22 deg·cm^2·dmol^{-1} for the maximum at ~225 nm. In addition, the zero crossings shifted to longer wavelengths with the decrease of carbohydrate content, reflecting a transition from a structured to a less structured conformation.[48] These data documented that the carbohydrate side chains reinforced the PPII configuration, in agreement with the higher PPII content found in FII compare to FIII.

Regarding the number of amino acid residues, a polypeptide backbone length >400 residues for the GAGP fraction and a rodlike structure of 150-nm long and 5-nm diameter was found.[22] In addition, the molecular weight of this GAGP fraction was estimated to be of 2.2×10^5 g/mol. A recent study dealing with hydroxyproline-rich glycoproteins from *Chlamydomonas reinhardtii* showed that one glycoprotein domain adopted an uniform left-handed PPII helix, wherein 1 nm of the extended configuration corresponded to 3.34 amino acids.[48] The domain constituted of 165 amino acids would translate into a 50-nm rod. Taking this result into consideration, the GAGP molecular fraction of 150-nm long[22] would be composed of ~495 residues. Refinement of the GAGP structure, based on the hydroxyproline contiguity and the extended polyproline II helix present in the molecule hypotheses, lead in fact to 380 residues (20 peptide repeats of a 19-residue consensus sequence).[49] The amino acids quantification of the present study, based on biochemical analyses and molecular determinations using HPSEC-MALLS, would indicate that FII and FIII would be composed of several glycoprotein domains. This glycoprotein subunits assembly would be compatible with the "abnormal" values found for the number of residues in each molecular fraction compared to literature data. In addition, the 43 residues calculated for FI was in reasonable agreement with the 19-residue consensus sequence[49] repeated twice.

Intrinsic Fluorescence. The third spectroscopic characterization of Acacia gum and its fractions dealt with intrinsic

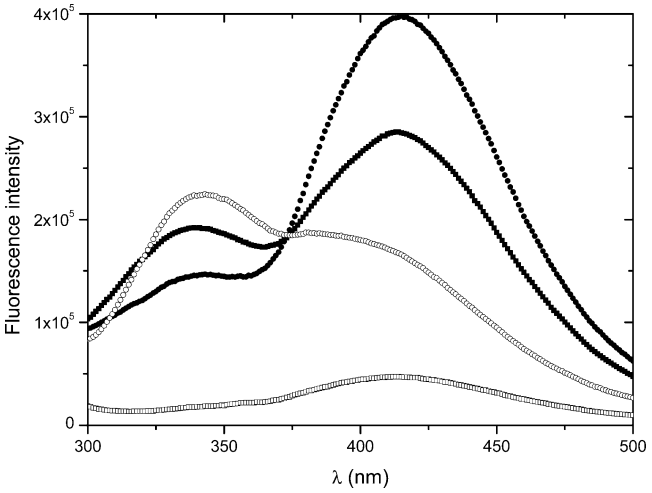

Figure 8. Fluorescence spectra of Acacia gum ($C = 4\%$, w/v) and molecular fractions I ($C = 4\%$, w/v), II ($C = 0.7\%$, w/v), and III ($C = 0.3\%$, w/v) solutions in water obtained after hydrophobic interaction chromatography; excitation wavelength 290 nm. (■) total gum, (□) fraction I, (●) fraction II, and (○) fraction III

fluorescence spectroscopy in order to probe the local structure of these hydroxyproline-rich heteropolysaccharides in the vicinity of aromatic amino acids and, in particular, tryptophan (Trp) residues. It was first checked that the fluorescence intensity, after excitation at $\lambda = 290$ nm, was linear with the Acacia gum concentration in the 0.25−20 wt % concentration range (data not shown). However, the wavelength at which the fluorescence emission maximum appeared shifted toward higher value with increasing gum concentration (i.e., from 342 to 345 nm in the concentration range tested). Figure 8 displayed fluorescence emission spectra of Acacia gum and its fractions after excitation at $\lambda = 290$ nm. The excitation wavelength was chosen in order to get intrinsic fluorescence emission from Trp residues, the fluorescence from phenylalanine and tyrosine being negligible at this wavelength.[50] It was first noticed that the fluorescence emission evolved as a function of time; an average intensity, based on four spectra taken at different time intervals, was thus calculated for each sample. In addition, the fluctuations in fluorescence intensity measured as a function of time was independent of the excitation wavelength used (280, 290, or 330 nm). A blue shift in the Trp emission was observed for total gum, FII, and FIII relative to the emission of Trp alone in water. The emission maximum was located at 341, 343.5, and 344 ± 1 nm for respectively total gum, FII, and FIII compared to 348 nm for the emission of Trp alone in water. This blue shift would be the result of exposed tryptophanyl residues to the solvent from the heteropolysaccharide structures, the unmasking effect of these aromatic residues being the most pronounced in FIII. This surprising result, considering the hydrophobic nature of Trp residues, would be related to the peculiar structure of FII and FIII and, in particular, the PPII type conformations and unordered structures predicted from circular dichroism spectra. The absence of maximum in the fluorescence emission spectrum of FI would reflect the absence of Trp residues or their highly buried location in the molecule. The emission spectrum of FI in the presence of 8 M urea revealed no maximum and confirmed the absence of Trp residues in FI (data not shown).

A second emission maximum was noticed at longer wavelengths for Acacia gum, FI, and FII. This emission maximum was located at 414, 413, and 415 nm for total gum, FI, and FII, respectively, whatever the excitation wavelength used (280, 290, or 330 nm). No maximum was clearly identified in the spectrum of FIII, the fluorescence intensity being however higher than in the FI case. The presence of a residual absorbance in the UV−Vis spectra of total gum, FII, and FIII near 330 nm (see Figure 6) was exploited here where the fluorescence emission intensity was recorded after excitation to $\lambda = 330$ nm. Emission spectra were similar to those recorded after excitation to $\lambda = 290$ nm with a slight shift however toward higher wavelength of the emission maximum (data not shown). In addition, a shoulder with a maximum located at $\lambda = 402$ nm was identified in FIII spectrum.

The most probable phenolic compounds that are largely encountered in plants, in particular cell walls, and that give intrinsic fluorescence after excitation at the appropriate wavelength are hydroxycinnamic acids: coumaric, caffeic, ferulic, and sinapic acids.[51] These phenolic compounds absorb the UV−B radiation (280−315 nm), with a maximum absorbance for *trans*-caffeic acid and *trans*-ferulic acid located at 329 and 325 nm, respectively.[52] The fluorescence emission maximum of caffeic and ferulic acids, after excitation at $\lambda = 330$ nm, is located at 425 and 415 nm, respectively.

Our UV absorbance and intrinsic fluorescence emission data would be more in agreement with the presence of ferulic acid in the molecular fractions of Acacia gum. This hypothesis was checked through the phenolic compounds identification and quantification where traces of trans ferulic acid and ferulic acid were found in Acacia gum (data not shown). In addition, traces of 8−5′ non cyclic diferulic acid was found in FII (13−15 ng/g). Even if a slight maximum in fluorescence intensity was measured in the case of FI, no phenolic compounds could be detected by HPLC. The versatile intensities measured in the molecular fractions fluorescence spectra could be related to the isomerization cis-trans occurring within these phenolic compounds as a function of time or pH. It was demonstrated for instance that fluorescence with emission wavelength $\lambda_{em} = 460$ nm and excitation wavelength $\lambda_{exc} = 390$ nm observed from caffeic acid in alkaline solution was attributed to the ionized phenolate ions (i.e., cis form), whereas fluorescence with $\lambda_{em} = 425$ nm and $\lambda_{exc} = 330$ nm in acidic solutions originated from the protonated phenolic form of caffeic acid (i.e., trans form).[53] The question arising from our results would be to know if ferulic acid monomer and dimer identified by HPLC are ester-linked to FII as it is classically found within the cell wall polymers. Sugars such as arabinose and xylose were found to be easily acylated by the carboxylic group of ferulic acid giving rise to feruloylated saccharides and allowing cross-links between oligosaccharides within the cell wall.[51] Isolation of diferulic bridges ester-linked to arabinan in sugar beet cell walls was also recently identified.[54] From the extensive dialysis performed to get Acacia gum and its molecular fractions, it would be reasonable to assume that these phenolic compounds are covalently linked to the heteropolysaccharides. Further studies and in particular mass spectrometry would be necessary to elucidate the fine structure of the covalent links between phenolic compounds and sugar residues contained in Acacia gum.

Fourier Transform Infrared Spectroscopy. Acacia gum and its fractions were analyzed in their solid state in order to be unaffected by the strong water absorption in particular in the amide I band region (1720−1580 cm^{-1}) characteristic of vibrations of peptidic bonds. Figure 9 displayed infrared spectra of Acacia gum and its fractions between 2000 and 800 cm^{-1} highlighting the major spectral bands attributed to protein and carbohydrate moieties. It was identified that the IR bands of

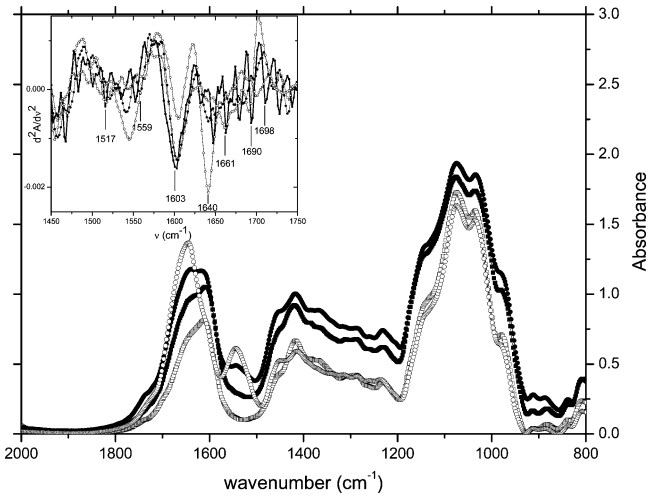

Figure 9. Infrared spectra of acacia gum, molecular fractions I, II, and III obtained after hydrophobic interaction chromatography in their solid state. (■) Total gum, (□) fraction I, (●) fraction II, and (○) fraction III. Inset: second derivative spectra associated to vibrational amide I and II bands (1750−1450 cm^{-1})

β-(1 → 6) or β-(1 → 3)-linked galactan occurred at about 1078−1072 cm^{-1}, whereas the main chain forming arabinan was at 1039 cm^{-1}.[55] In addition, COO^- asymmetric stretching bands located at 1420 and 1454 cm^{-1} and CH_2 esters bending vibrational bands around 1300 cm^{-1} were also identified in all of the samples with the strongest bands for FII. The methyl group substitution ($COO-CH_3$) allowing the substitution degree to be determined was clearly seen at 980 cm^{-1} whatever the sample, the strongest band being also for FII.

The polypeptidic backbone constitutive of Acacia gum and its fractions was identified by the intense amide I band at 1600−1650 cm^{-1} and the less intense amide II band at 1540−1550 cm^{-1}. Second derivative spectra of amide I and II bands allowed both better resolution of overlapping spectral components and qualitative analysis of secondary structures (inset Figure 9). The second derivative spectra validated the presence of extended β-sheets (presence of the strong bands at 1640 cm^{-1}) in all molecular fractions. In addition, presence of the band at 1690 cm^{-1} suggested the presence of β-turns in the three molecular fractions. The band at 1661 cm^{-1} identified in Acacia gum and FI was also attributed to β-turns. The band at 1698 cm^{-1} identified in FI and FII was assigned to the side chain absorbance of solvent exposed aspartic (Asp) and glutamic (Glu) acids COOH modes. The shoulder at 1559 cm^{-1} identified in FII corresponded to stretching vibrations of COO^- of Glu residues. Finally, the band at 1517 cm^{-1} identified in the three molecular fractions was attributed to surfacing of tyrosine residues. It also appeared clearly from IR second derivative spectra of Acacia gum molecular fractions that the characteristic band assigned to α-helices at 1650 cm^{-1} was totally absent.

Polyelectrolyte Behavior of Total Acacia Gum and Its Molecular Fractions. Acidic forms of Acacia gum and its fractions were titrated using 0.01 N NaOH solution. The relationships between pK_a and the degree of dissociation α of Acacia gum, FI, FII, and FIII are displayed in Figure 10. The main charged monomers, glucuronic (GlcUA), aspartic (Asp), and glutamic (Glu) acids, were also displayed for comparison. A pK_a increase occurred with the increase of α in Acacia gum and its fractions contrary to what was observed for simple electrolyte such as GlcUA, Asp, and Glu. pK_a curves of the single charged monomers GlcUA, Asp, and Glu were independent of the degree of dissociation α; linear extrapolation to zero degree of dissociation gave pK_0 values of 3.06 ± 0.04, 3.63 ± 0.02, and 4.26 ± 0.03 for GlcUA, Asp, and Glu, respectively. pK_a curves of Acacia gum and its fractions revealed a monotonic quasi-linear dependence with the degree of dissociation α characteristic of low charge density polymers of polyelectrolyte behavior. In addition, the slope of the p$K_a = f(\alpha)$ dependence was the highest in FII, the slope value being characteristic of a weak poly-acid. These results would indicate that the dissociation of each charged group depended on the degree of dissociation of neighboring charges. The intense electrostatic potential surrounding the polymer would markedly affect the counterions distribution and would provoke a pK_a dependence with the degree of dissociation α. Theoretical treatment classically ascribed to linear polyelectrolyte chain such as Lifson and Katchalsky theory[56] failed in the particular case of weakly charged polyelectrolytes for which the uniformly charged-rod model is incorrect as long as the distance between two sites is larger than about 0.7 nm.[57] In addition, in the particular case of molecular fractions purified from Acacia gum, charges came from GlcUA but also from acid (Asp and Glu) and basic (Arg, Lys, and Tyr) amino acids. As a consequence, data fitting to extract pK_0 values of both each molecular fraction was only performed using a linear regression fitting procedure. It was checked that the same results were also obtained by using a second degree polynomial function (data not shown). Acacia gum, FI, FII, and FIII had pK_0 values of 3.58 ± 0.02, 3.78 ± 0.02, 2.70 ± 0.01, and 4.20 ± 0.04, respectively. These pK_0 values were much higher than those found for GlcUA except for FII where the intrinsic pK of the polymer was much lower than those determined for the simple electrolytes GlcUA, Asp, and Glu. These findings indicated clearly both contributions of charged sugar residues and amino acids in the polyelectrolyte behavior of Acacia gum and its fractions. To gain deeper insight into the charge distributions on each molecular fraction, calculations were performed, based on the sugar and protein molar composition, to determine the number of GlcUA residues. In addition, the number of total charges (GlcUA residues and charged amino acids) was calculated from the number of moles of OH^- necessary to neutralize the mass of each fraction used for titration experiments. The charge distributions coming from polysaccharidic substitutions and polypeptidic backbone on each fraction were thus deduced from the difference in the number of charges identified by each method. Table 6 summarized the number of charges and charge distributions on each fraction resulting from biochemical and titration analyses. It was thus found that the charges distribution in FI solely came from polysaccharidic substitutions (GlcUA brought 100% of total charges). In agreement with the increase of protein content in FII and FIII, charges distribution came from the polypeptidic backbone at a level of 8.7% and 62.1%, respectively. In the particular case of Acacia gum, the number of charges calculated from titration experiments was lower than those found from biochemical composition. This discrepancy between the two methods used to calculate the number of charges could result from aggregation phenomena occurring in the starting material during titration experiments. The consequence of Acacia gum aggregation on charges determination would be that part of the charges brought by the aggregates would not be accessible to OH^- counterions during titration experiments. From the electrometric titration of gum arabic solution, Acharya and Chattoraj clearly demonstrated the changes in the radius of the macroion as a function of pH, ionic strength, and temperature.[58] The authors also added that the discrepancy found between the radius

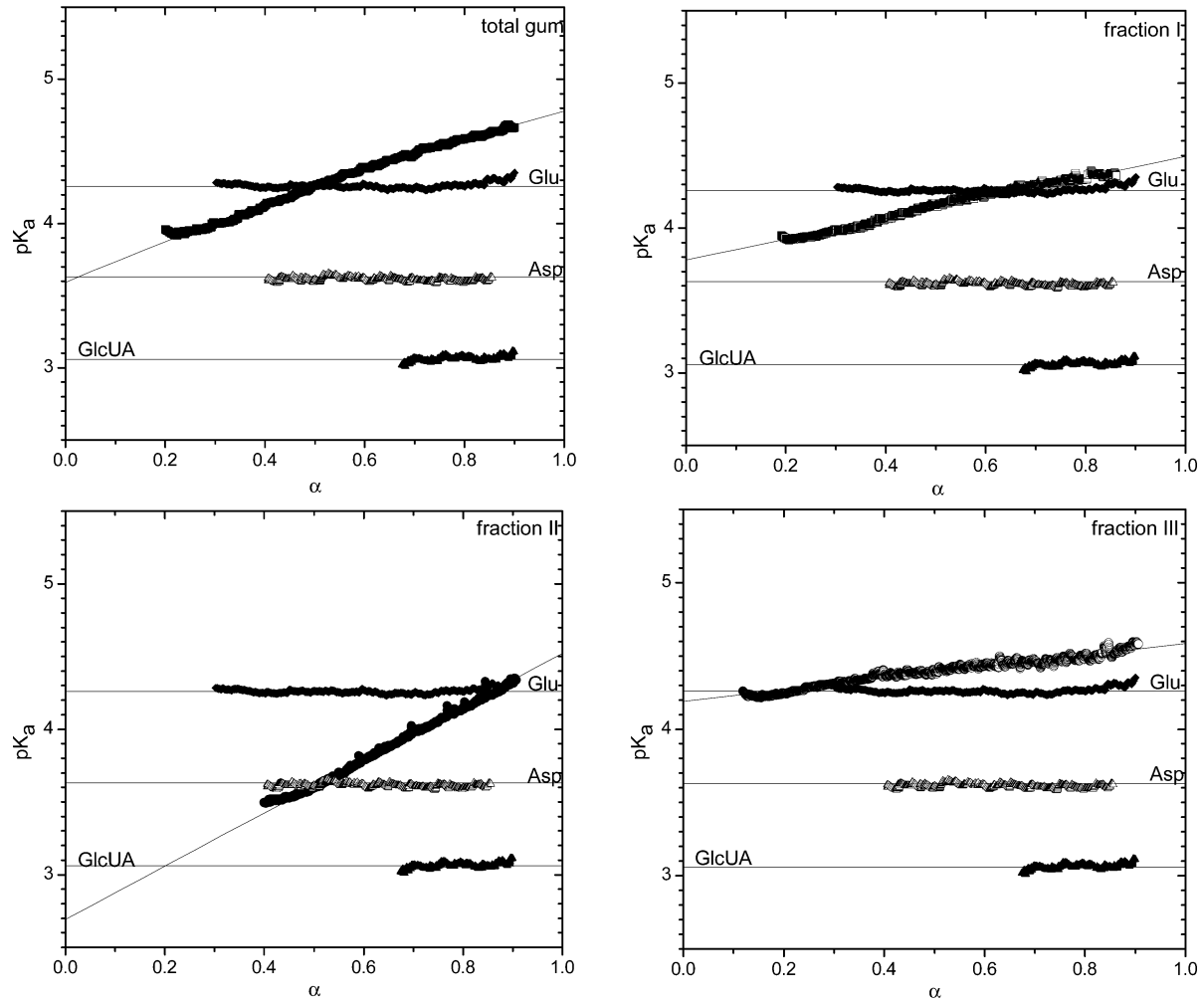

Figure 10. Variations in pK_a with the degree of dissociation α of Acacia gum and its molecular fractions obtained after hydrophobic interaction chromatography. Glucuronic (GlcUA), aspartic (Asp), and glutamic (Glu) acids were also displayed for comparison. The lines were the corresponding theoretical functions using a second degree polynomial or a linear function. (■) Total gum, (□) fraction I, (●) fraction II, (○) fraction III, (▲) GlcUA, (△) Asp, (◆) Glu.

Table 6. Number of Charges and Charges Distribution on Acacia Gum and Its Molecular Fractions (Collected after Hydrophobic Interaction Chromatography) Calculated from Biochemical Composition (Glucuronic Acid Residues, GlcUA) and Titration Data (GlcUA + Charged Amino Acids)[a]

		fraction		
number of charges	total gum	I	II	III
from biochemistry				
glucuronic acid (GlcUA)	402	223	1149	609
from titration				
glucuronic acid (GlcUA) + charged amino acids	368	223	1259	1605
charges distribution				
polysaccharidic substitutions		100%	91.3%	37.9%
polypeptidic backbone		0%	8.7%	62.1%

[a] See text for details.

of the polyion determined from both titration and viscosity data could be related to the nonuniform charge distribution throughout the surface or volume of the macromolecule. Even if this argument is probably true, aggregation phenomena in Acacia gum may be questioned considering the huge differences the authors found in the radius of Acacia gum as a function of pH and temperature. Further experimental details, in particular three-dimensional structure of each molecular fraction found in Acacia gum, would be necessary to get a better idea of the polypeptide backbone and polysaccharidic substitutions spatial positions and consequently charge distributions throughout each heteropolysaccharide.

4. Conclusion

Fractionation of *Acacia senegal* gum using hydrophobic interaction chromatography revealed three main molecular fractions, and both biochemical and physicochemical analyses confirmed the existence of an arabinogalactan-peptide (FI), an arabinogalactan-protein (FII), and a glycoprotein (FIII) fraction. FIII, after new purification using size exclusion chromatography, was found to be a highly polymolecular and polydisperse fraction where a continuum of molecular species differing both by the protein-to-sugar ratio and molecular weight was identified. From literature data, one polypeptidic backbone would be present in each molecular fraction whose length determined in the present study was of 43, 2253, and 4443 amino acid residues in FI, FII, and FIII, respectively. It maybe questioned however if only one polypeptidic backbone would exist in FII and FIII fractions considering both higher number of residues found compared to literature data and different populations determined through HPSEC-MALLS characterization. Secondary structure predictions in FII and FIII revealed the presence of polyproline II type helices, β-sheets, and random coils structures. From the relative exposition of certain hydrophobic aromatic amino acid

residues to solvent (i.e., Trp and Tyr), a relevant structural investigation of each molecular fraction using scattering techniques and mass spectrometry would be useful to elucidate the spatial arrangement of the polypeptidic backbone and the polysaccharidic substitutions in these complex heteropolysaccharidic structures. These future structural investigations would highlight the biological and/or functional role of each molecular fraction contained in Acacia gum.

Acknowledgment. We are grateful to Marie-Jeanne Crepeau for her technical assistance during chromatographic experiments and to Dr. Christophe Schmitt for fruitful discussions and critical comments on this work.

References and Notes

(1) Verbeken, D.; Dierckx, S.; Dewettinck, K. *Appl. Microbiol. Biotechnol.* **2003**, *63*, 10−21.
(2) Snowden, M. J.; Phillips, G. O.; Williams, P. A. *Food Hydrocolloids* **1987**, *1*, 291−300.
(3) Whistler, R. L. In *Industrial gums: Polysaccharides and their derivatives*; Whistler, R. L., Bemiller, J. N., Eds.; Academic Press: San Diego, 1993; pp 309−339.
(4) Phillips, G. O.; Williams, P. A. In *Ingredient interactions-effects on food quality*; Gaonkar, A. G., Ed.; Marcel Dekker: New York, 1995; pp 131−169.
(5) Phillips, G. O. *Food Addit. Contam.* **1998**, *15*, 251−264.
(6) Buffo, R.; Reineccius, G. *Perfumer Flavorist* **2000**, *25*, 24−44.
(7) Burgess, D. J.; Carless, J. E. *J. Colloid Interface Sci.* **1984**, *88*, 1−8.
(8) Schmitt, C.; Sanchez, C.; Despond, S.; Renard, D.; Thomas, F.; Hardy, J. *Food Hydrocolloids* **2000**, *14*, 403−413.
(9) Trindade, M. A.; Grosso, C. R. F. *J. Microencapsulation* **2000**, *17*, 169−176.
(10) Jouzel, B.; Pennarun, A.-L.; Prost, C.; Renard, D.; Poncelet, D.; Demaimay, M. *J. Microencapsulation* **2003**, *20*, 35−46.
(11) FAO. Gum arabic. (Food and nutrition paper 52, addendum 7) *FAO*, 1999, Rome.
(12) Anderson, D. M. W.; Stoddart, J. F. *Carbohydr. Res.* **1966**, *2*, 104−114.
(13) Churms, S. C.; Merrifield, E. H.; Stephen, A. M. *Carbohydr. Res.* **1983**, *123*, 267−279.
(14) Anderson, D. M. W.; Bridgeman, M. M. E.; Farquhar, J. G. K.; McNab, C. G. A. *Int. Tree Crops J.* **1983**, *2*, 245−254.
(15) Vandevelde, M. C.; Fenyo, J. C. *Carbohydr. Polym.* **1985**, *5*, 251−273.
(16) Randall, R. C.; Phillips, G. O.; Williams, P. A. *Food Hydrocolloids* **1988**, *2*, 131−140.
(17) Randall, R. C.; Phillips, G. O.; Williams, P. A. *Food Hydrocolloids* **1989**, *3*, 65−75.
(18) Osman, M. E.; Menzies, A. R.; Martin, B. A.; Williams, P. A.; Phillips, G. O.; Baldwin, T. C. *Phytochemistry* **1995**, *38*, 409−417.
(19) Islam, A. M.; Phillips, G. O.; Sljivo, A.; Snowden, M. J.; Williams, P. A. *Food Hydrocolloids* **1997**, *11*, 493−505.
(20) Williams, P. A.; Phillips, G. O.; Stephen, A. M. *Food Hydrocolloids* **1990**, *4*, 305−311.
(21) Fincher, G. B.; Stone, B. A.; Clarke, A. E. *Annu. Rev. Plant Physiol.* **1983**, *34*, 47−70.
(22) Qi, W.; Fong, C.; Lamport, D. T. A. *Plant Physiol.* **1991**, *96*, 848−855.
(23) Sanchez, C.; Renard, D.; Robert, P.; Schmitt, C.; Lefebvre, J. *Food Hydrocolloids* **2002**, *16*, 257−267.
(24) López-Franco, Y. L.; Valdez, M. A.; Hernández, J.; Calderón de la Barca, A. M.; Rinaudo, M.; Goycoolea, F. M. *Macromol. Biosci.* **2004**, *4*, 865−874.
(25) Schmitt, C. Ph.D. Thesis, INPL, Vandoeuvre-lès-Nancy, France, 2000.
(26) Thibault, J.-F. *Lebens.-Wissen. Technol.* **1979**, *12*, 247−251.
(27) Tollier, M.-T.; Robin, J.-P. *Ann. Technol. Agric.* **1979**, *28*, 1−15.
(28) Blakeney, A. B.; Harris, P. J.; Henry, R. J.; Stone, B. A. *Carbohydr. Res.* **1983**, *113*, 291−299.
(29) Wall, L. L.; Gehrke, C. W. *J. AOAC* **1975**, *58*, 1221−1226.
(30) Bidlingmeyer, B. A.; Cohen, S. A.; Tarvin, T. L. *J. Chromatogr.* **1984**, *336*, 93−104.
(31) Saulnier, L.; Crépeau, M.-J.; Lahaye, M.; Thibault, J.-F.; Garcia-Conesa, M. T.; Kroon, P. A.; Williamson, G. *Carbohydr. Res.* **1999**, *320*, 82−92.
(32) Deléage, G.; Geourjon, C. *CABIOS* **1993**, *9*, 197−199.
(33) Sreerama,, N.; Woody, R. W. *Anal. Biochem.* **1993**, *209*, 32−44.
(34) Osman, M. E.; Menzies, A. R.; Williams, P. A.; Phillips, G. O.; Baldwin, T. C. *Carbohydr. Res.* **1993**, *246*, 303−318.
(35) Ray, A. K.; Bird, P. B.; Iacobucci, G. A.; Clark, B. C., Jr. *Food Hydrocolloids* **1995**, *9*, 123−131.
(36) Du, H.; Clarke, A. E.; Bacic, A. *Trends Cell Biol.* **1996**, *6*, 411−414.
(37) Williams, P. A.; Langdon, M. J. *Chromatogr. Anal.* **1995**, *October/November*, 5−7.
(38) Idris, O. H. M.; Williams, P. A.; Phillips, G. O. *Food Hydrocolloids* **1998**, *12*, 379−388.
(39) Picton, L.; Bataille, I.; Muller, G. *Food Hydrocolloids* **2000**, *42*, 23−31.
(40) Al-Assaf, S.; Phillips, G. O.; Williams, P. A. *Food Hydrocolloids* **2005**, *19*, 647−660.
(41) Gerle, M.; Fischer, K.; Roos, S.; Müller, A. H. E.; Schmidt, M. *Macromolecules* **1999**, *32*, 2629−2637.
(42) Heckman, J. W., Jr.; Terhune, B. T.; Lamport, D. T. A. *Plant Physiol.* **1988**, *86*, 848−856.
(43) Veis, A.; Eggenberger, D. N. *J. Am. Chem. Soc.* **1954**, *76*, 1560−1563.
(44) Homer, R. B.; Roberts, K. *Plant Physiol.* **1979**, *146*, 217−222.
(45) Zhao, Z. D.; Tan, L.; Showalter, A. M.; Lamport, D. T. A.; Kieliszewski, M. J. *Plant J.* **2002**, *31*, 431−434.
(46) Tan, L.; Qiu, F.; Lamport, D. T. A.; Kieliszewski, M. J. *J. Biol. Chem.* **2004**, *279*, 13156−13165.
(47) Shpak, E.; Barbar, E.; Leykam, J. F.; Kieliszewski, M. J. *J. Biol. Chem.* **2001**, *276*, 11272−11278.
(48) Ferris, P. J.; Woessner, J. P.; Waffenschmidt, S.; Kilz, S.; Drees, J.; Goodenough, U. W. *Biochemistry* **2001**, *40*, 2978−2987.
(49) Goodrum, L. J.; Patel, A.; Leykam, J. F.; Kieliszewski, M. J. *Phytochemistry* **2000**, *54*, 99−106.
(50) Lakowicz, J. R. In *Principles of fluorescence spectroscopy*; Lakowicz, J. R., Ed.; Plenum Press: New York, 1983; pp 341−381.
(51) Mathew, S.; Abraham, T. E. *Crit. Rev. Biotechnol.* **2004**, *24*(2−3), 59−83.
(52) Kolb, C. A.; Pfündel, E. E. *Plant, Cell Environ.* **2005**, *25*, 580−590.
(53) Smith, G. J.; Haskell, T. G. *J. Photochem. Photobiol.* **2000**, *55*, 103−108.
(54) Levigne, S.; Ralet, M.-C.; Quéméner, B.; Thibault, J.-F. *Carbohydr. Res.* **2004**, *339*, 2315−2319.
(55) Kaèuráková, M.; Capek, P.; Sasinková, V.; Wellner, N.; Ebringerová, A. *Carbohydr. Polym.* **2000**, *43*, 195−203.
(56) Lifson, S.; Katchalsky, A. *J. Polym. Sci.* **1954**, *13*, 43−55.
(57) Rinaudo, M.; Milas, M. *J. Polym. Sci.* **1974**, *12*, 2073−2081.
(58) Acharya, L.; Chattoraj, D. K. *Ind. J. Chem.* **1975**, *13*, 564−568.

BM060145J